DOE/PC/89776--T8

3rd QUARTERLY PROJECT STATUS REPORT

Project Title:
Effects of Calcium Magnesium Acetate on the Combustion of Coal-Water Slurries

DOE/PC/89776--T8

DE92 018313

DOE Grant #: DE-FG22-89PC89776

Principal Investigator: Yiannis A. Levendis

Project Period: 1 March 1990 - 31 May 1990

Project Objectives:

The general objective of the project is to investigate the combustion behavior of single and multiple Coal-Water Slurry particles burning at high temperature environments. Both uncatalyzed as well as catalyzed CWS drops with Calcium Magnesium Acetate (CMA) catalyst will be investigated. Emphasis will also be given in the effects of CMA on the sulfur capture during combustion. To help achieve these objectives the following project tasks were carried over this 3*rd* three-month period.

Project Tasks:

1 MODELLING OF THE EVAPORATION AND HEAT-UP PERIODS FOR COAL-WATER SLURRIES.

A. Pure Water Droplets.

For a coal-water slurry droplet a knowledge of the evaporation time and axial position in the furnace at the end of the evaporation phase is required. This information cannot be obtained using the present experimental setup. Thus, calculation schemes were used to obtain the drop history throughout the evaporation phase, a simplified analytical method and two numerical schemes. Gas phase conditions must be chosen before introduction of a dispersed phase (droplet). Calculations were performed with injector flowrates set to 0.1 lpm.

where velocity and temperature profiles are disturbed minimally by the injector flow. Initial droplet diameters of 50 and 250 μm were chosen as this is the size targeted for combustion experiments.

Analytical Solution. This is essentially a solution for a stationary droplet in an unbounded medium with a constant bulk gas temperature and a constant drop surface temperature. Modelling of drop evaporation has been extensively analyzed by Faeth[17], Sirignano[18] and Lefebrve[19] who has also made an extensive review of such models. The following d^2 law has been used in the model:

$$d_0^2 - d^2 = \lambda t \tag{1}$$

where d is the drop diameter. Steady-state evaporation (i.e. a quasi-steady gas phase) was assumed for the total drop lifetime. Assuming a Lewis number of unity it can be shown that

$$\lambda = \frac{8k_g \ln(1+B)}{c_{p_g}\rho_p} \tag{2}$$

The heat transfer number B was obtained using an iterative method described by Spalding [20] and Kanury [21]. The evaporation constant, λ, was then calculated using Eq. 2 and substituted into Eq. 1 to give the drop diameter as a function of time.

Numerical Solutions The trajectory of the particle or droplet was obtained by solving the equations of motion including the effects of drag and gravity. The gas velocities were derived from the gas phase solution in the finite difference cell through which the particle was travelling. Heat and mass transfer from the droplet were computed at each time step to obtain its size and temperature history. Heat and mass transfer coefficients were calculated using Nusselt type correlations. The rate of evaporation was computed first using the mass transfer coefficient and the partial pressure at the droplet surface and in the bulk gas phase. The partial pressure at the surface was assumed to be the vapour pressure at the droplet temperature from the previous time step. Then an energy balance was performed to update the particle temperature. This energy balance for the droplet included convective and latent

heat contributions, but the radiative heating term was neglected. The coupling of the two phases was continued until a converged solution was obtained for both phases. Numerical results were computed by the FLUENT software with continuous coupling with the gas phase and contrasted with a numerical scheme we developed, as described below, at constant gas temperature. The agreement was very good.

second numerical solution was obtained with a computer code developed by Levendis [Ph.D. Thesis, CALTECH 1988] described below. This algorithm assumes average gas properties instead of continuously updating the local gas environment conditions as FLUENT does. Again the agreement with the analytical solution was very good (within a few percent).

The theoretical formulation of the problem concerning the drying of liquid drops of diameter d and mass m should take into account the diffusional mass transfer of vapors from the particle to its surroundings and the unsteady particle temperature history:

$$\frac{dm}{dt} = -2\pi \left(\frac{6m}{\rho_{drop}\pi}\right)^{1/3} \rho_g D 18/29 (X_s - X_\infty) \tag{3}$$

$$dX/dt = -\frac{N}{\rho_g Q}\frac{dm}{dt} \tag{4}$$

$$\frac{dT}{dt} = \frac{1}{c_{drop} m}\left(\frac{dm}{dt}(c_{drop}T + H_0) + h\pi\left(\frac{6m}{\rho_{drop}\pi}\right)^{2/3}(T - T_\infty)\right), \tag{5}$$

where ρ_g is the density of the gas, ρ_{drop} is the density of the drop, D is the bulk molecular diffusion coefficient, N is the excitation frequency of the aerosol generator which is also equal to the number of drops generated per second, and Q is the gas flowrate. c_{drop} is the heat capacity of the drop, H_0 is the latent enthalpy of vaporization of the solvent and h is the heat transfer coefficient calculated as follows:

$$h = Nu\frac{k}{d} \qquad \text{where the Nusselt number, } Nu = 2.0; \tag{6}$$

here k is the thermal conductivity of the gaseous phase. X_∞ is the mass fraction of the vapors in the surrounding gas and X_s is the mass fraction of

the saturated vapor at the surface of the drop and is related to the partial pressure by a constant based on the molecular weight of the diffusing species in Eq. 3. The partial pressure at the surface can be expressed in terms of temperature in an Arrhenius form. For example, for water :

$$p_s = \exp\left(-\frac{1/T - 2.7 \times 10^{-3}}{2.0 \times 10^{-4}}\right). \tag{7}$$

The above system of first-order differential equations was solved numerically using a fourth-order Runge-Kutta method with automatic step-size control.

Results obtained from the FLUENT software for a 50μm pure water droplet are presented in Figure 1. The droplet was injected 11.5 cm above the injector tip. Evaporation was completed while the droplet was still inside the water-cooled injector. The bulk gas temperature assumed for the analytical solution was 323 K inside the injector. Agreement between the analytical and numerical solutions was quite good. This is to be expected since the assumption of a stationary droplet in respect to the gas, in the former method, is fulfilled for small particles such as 50μm. Numerical results for a 250μm pure water droplet indicate that the drop evaporates after travelling a considerable distance inside the radiation cavity, at wall temp. of 1500 K, Fig. 1 and 2. To compare these results with the analytical solution an average bulk gas phase temperature of 1400 K was assumed since the droplet falls rapidly through the injector and enters the "hot zone" with very little change in size. The evaporation rates predicted by the numerical scheme were higher (shorter total evaporation times) than those of the analytical solution. This may attributed to the fact that for larger drops the contribution of the second term in the Nusselt number correlation ($Nu = 2.0 + 0.6\, Re_d^{1/2}\, Pr^{1/3}$) becomes significant. This term was not included in the analytical solution.

B. Slurry Drops

Numerically predicted histories of 50 and 250μm slurry drops are shown in Figure 2. The initial composition was set to 75% water and 25% solids. Upon completion of the evaporation phase the particle temperature increases rapidly to the prevailing gas temperature. Droplet diameter-time and temperature-time plots are shown in Figures 3 and 4. The results show that the combustion

of the solid particles, remaining upon water evaporation from CWS drops, will take place at axial locations within the combustor that vary with the initial diameter of the droplet. The larger the initial drop the further down in the furnace the remaining solid is going to burn. Thus, modelling of the combustion of slurry requires a complete knowledge of gas phase environment. Results on Figs. 3 and 4 show that, under the conditions examined, evaporation for the 50μm takes 0.58 sec inside the injector, and for the faster falling 250μm takes a total of only 0.19 sec. inside both the injector and the radiation cavity. This is a rather interesting result. Information about the solid particle heatup times, upon completion of the evaporation, can be obtained from Figure 4. The 50 μm particles heats up to 1350 K in less than 0.1 sec. after it exits the injector and then follows the local gas temperature; the asymptotic gas temperature (1450 K) is reached in 2.0 sec. after completion of evaporation. The fast falling 250 μm particle reaches 1450 K within 0.15 sec after evaporation.

Future plans include the investigation of more droplet sizes as well as Coal-Ethanol mixtures.

2 PRODUCTION OF SINGLE DROPS

Work on developing techniques to produce single droplets of coal-water slurries has been continued over this period. Two different types of droplet generators have been under investigation: **(i)** one that utilizes mechanical means i.e. the action of a plunger to push a small quantity of slurry out of an orifice, and **(ii)** a generator that utilizes electrically driven piezoelectric transducers to generate a pressure wave and create a drop. We have assembled a working design of the former category shown in Fig. 5. The core element is supplied by *Xandex* and consists of a small cavity with a needle attached at the bottom. A thin plastic plunger is mounted at the centerline of the cavity and runs through the needle all the way to the bottom tip. Lifting the plunger, by spring motion from the top, slurry flows around the plunger to the space between the tip of the needle and the end of the plunger. Then application of a sudden force (impact) to the plunger expels a drop, Fig. 6. The size of the drops can be controlled by various diameters of needle-plunger combinations. The

technique is fairly repeatable but plugging becomes a problem occasionally. Photographs of generated drops are shown in Fig. 6. Drop size is 700μm, and 400μm in Figs. 6a and 6b, respectively.

The designs of three electrically driven generators were described in the 1st quarterly report (Dec. 1989); two out of those configurations have been constructed and tested. For all designs the basic principle is the same. a sudden construction of a piston or a wall of the fluid container creates an acoustic wave. This contraction or movement is produced when a DC voltage pulse with a short rise time, is applied to a piezoelectric transducer. The wave travels through the fluid until it strikes a small orifice. If a pressure sufficient to overcome surface tension at the orifice is created and enough fluid displacement is generated a drop will be ejected from the main body of the fluid.

CONFIGURATION #1. In this design two rectangular piezoelectric bimorph elements (0.25 mm thick) were glued to both sides of a flattened copper tube with a conductive silver epoxy. The maximum displacement is obtained with a bimorph by making the length to thickness ratio of the bimorph as high as possible. However, this also means that the maximum field (5 V/25μm) that can be applied without permanent depolarization is easily reached. This design failed to produce drops. A possible explanation of the failure of this design is that the displacement of the wall of the copper tube is reduced because the epoxy layer acts as a cushion between the bimorph and the tube wall. Also the copper tube has a certain rigidity which will resist any inward motion of the bimorph. A possible improvement might consist of constraining the outside of the piezoelectric with a rigid wall in order to maximize inward displacement. However, further developmental work with this design is not planned. The restrictions on the movement of the piezoelectric transducer, inherent in this design, and the low field depolarization limit suggest that this design is not suitable for generating the higher pressures and displacements required to produce CWS droplets.

CONFIGURATION #2. In this design a piston attached to a 30 element stack piezoelectric actuator is used. Two variations of this design were built,

one with a piston seal and inlet and outlet tubes for filling and emptying (Fig. 7a), and the other with no inlet and outlet tubes but with a small clearance between the piston and the cylinder wall to allow air to leave the system after filling and insertion of the piston. The elements of the actuator are electrically in series but mechanically in parallel with a field depolarization limit of 100 volts pe· element. This indicates that much greater displacements should be possible than for configuration #1. However, the piston is glued to the actuator with an epoxy, which may again be acting as a cushion to reduce the actual displacement of the piston. The device is shown on Fig. 7b. Experiments to this date have been unsuccessful, nonetheless an experiment is planned to measure the piston displacement directly. It should be noted that while this design should give high displacements, the force exerted by the actuator is the same as that exerted by one element acting alone at the same voltage. This device is driven by a single pulse electrical signal generator, constructed for this purpose which is now capable of creating pulses having durations in the range of 1 ms to 1 sec, and amplitudes up to 100 V.

Future plans include improvements on the second design, construction of a third design to be driven by a piezoelectric bimorph and modification of all the above to be driven by mechanical impact.

3 DESIGN AND CONSTRUCTION OF A SYSTEM FOR PERFORMING OPTICAL OBSERVATIONS INSIDE THE FURNACE.

While our laminar flow, drop-tube furnace incorporates two side view ports major observations will be conducted from the top of the injector, along the centerline of the furnace. Viewing this way, one can monitor the complete burnout history of the solid particle from ignition to extinction. Thence, the light collection optical system must be situated at the top of the furnace injector. Furthermore at the top of the injector both the particle and drop generation systems must also be located. This of course creates a need for compromise in the utilization of the limited space since the inner diameter of the furnace injector is only 1.25 cm and particle injectors can obscure the

view. To minimize this problem particle/droplet injectors must be as small as possible, preferably less than 1 mm in diameter.

At the top of the furnace a collimating lens is needed to focus the light from burning particles on to one end of an optical fiber and transmit it to the optical pyrometer which is situated at the other end. The optical fiber serves as the coupling medium between the furnace and the pyrometer. A state of the art, 1 mm diameter, 1.6 m long single optical fiber, manufactured by *General Fiber Optic*, has been selected and purchased for this purpose. A single fiber optic has the advantage of maximizing the light transmission efficiency since all of its cross-section is been utilized. In contrast the cross-section of fiber bundles contains a lot of dead space between the individual fibers, thus, reducing the light collection efficiency. Furthermore, a split optical fiber bundle (bifurcated or trifurcated) was not chosen because, in addition to the the above reason, it introduces further uncertainties since, the fiber split in the bundle is random and there is not guarantee that the light will be equally divided among the channels.

Light from burning particles is seen by an inverted collimator (*ORIEL*, 11 mm diameter, 19 mm focal length lens) and is focused on the optical fiber, Fig. 8. The overall length of the 1.25 i.d. furnace injector was designed to be 61 cm so that the lens would not "see" any **direct** radiation from the furnace walls. To avoid *reflected* furnace radiation from climbing inside the injector (after multiple reflections on the inner walls) and reaching the optical fiber two precautions were taken (a) the injector was black passivated and (b) a pinhole was used between the lens and the fiber (Fig. 8) on the imaginary surface of the conical contour of the collimated rays to block any stray "reflected" rays. The pinhole can be placed at any position on the centerline between the lens and the fiber and should have a diameter equal to the cross section of the cone at that hight. A pinhole diameter of 0.5 mm was chosen which fixes its distance from the upper surface of the lens to 18.14 mm. The position of the lens is fixed but both the pinhole and the optical fiber can move axially relative to the lens and against each other. This allows for fine tuning of the

system during experiments. Fine motion is provided by two micropositioners (manufactured by *NEWPORT and ORIEL*) and depicted on Fig. 9.

Future plans include a three-color pyrometer which has been designed and is currently constructed. Detailed description will be given in the next report.

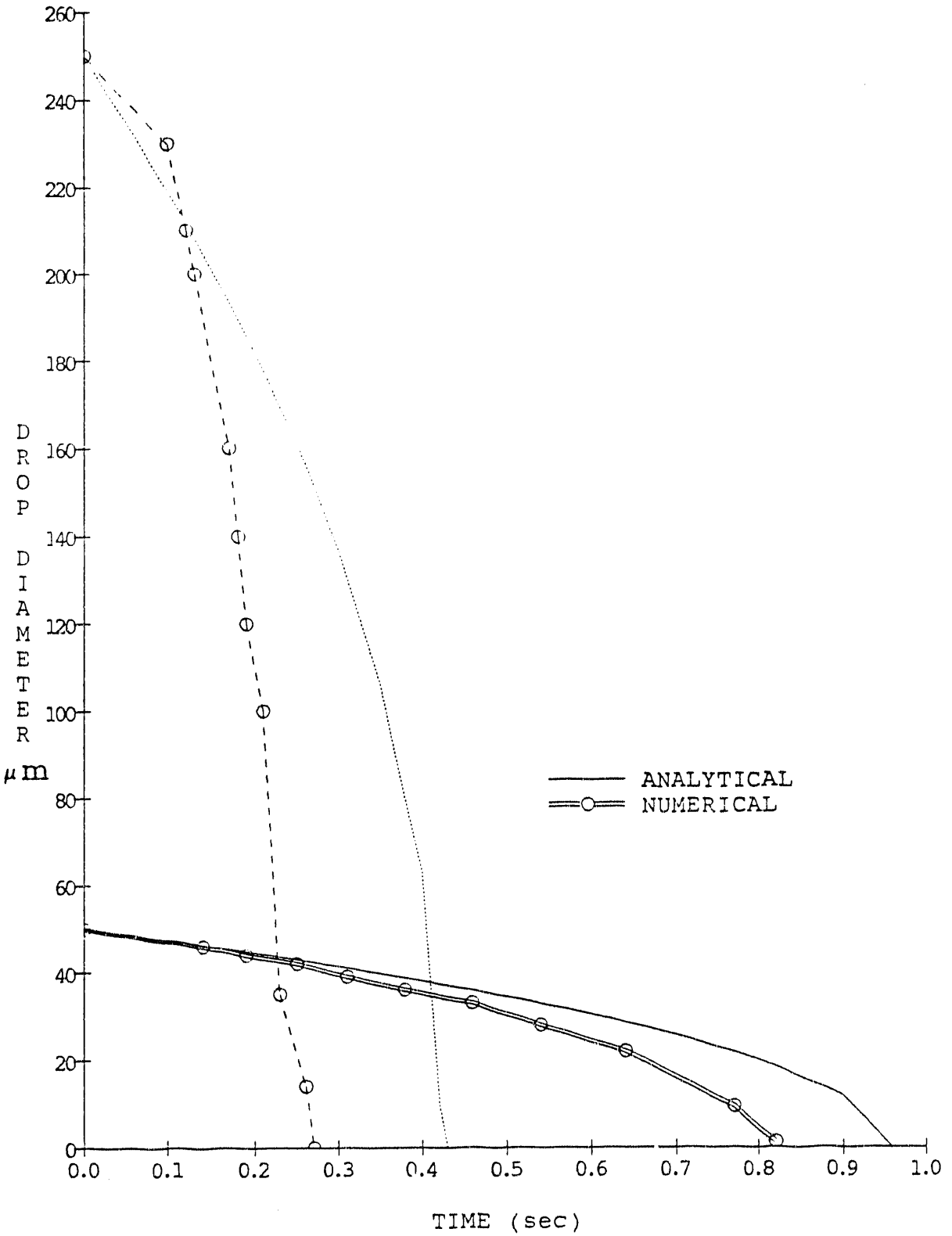

FIGURE 1. Analytical and numerical calculation of evaporating water droplet diameter as a function of time, for initial drop diameters of 50 and 250μm. Injector flowrate 0.1 lpm, furnace flowrate at 2.0 lpm, wall temperature 1500 K.

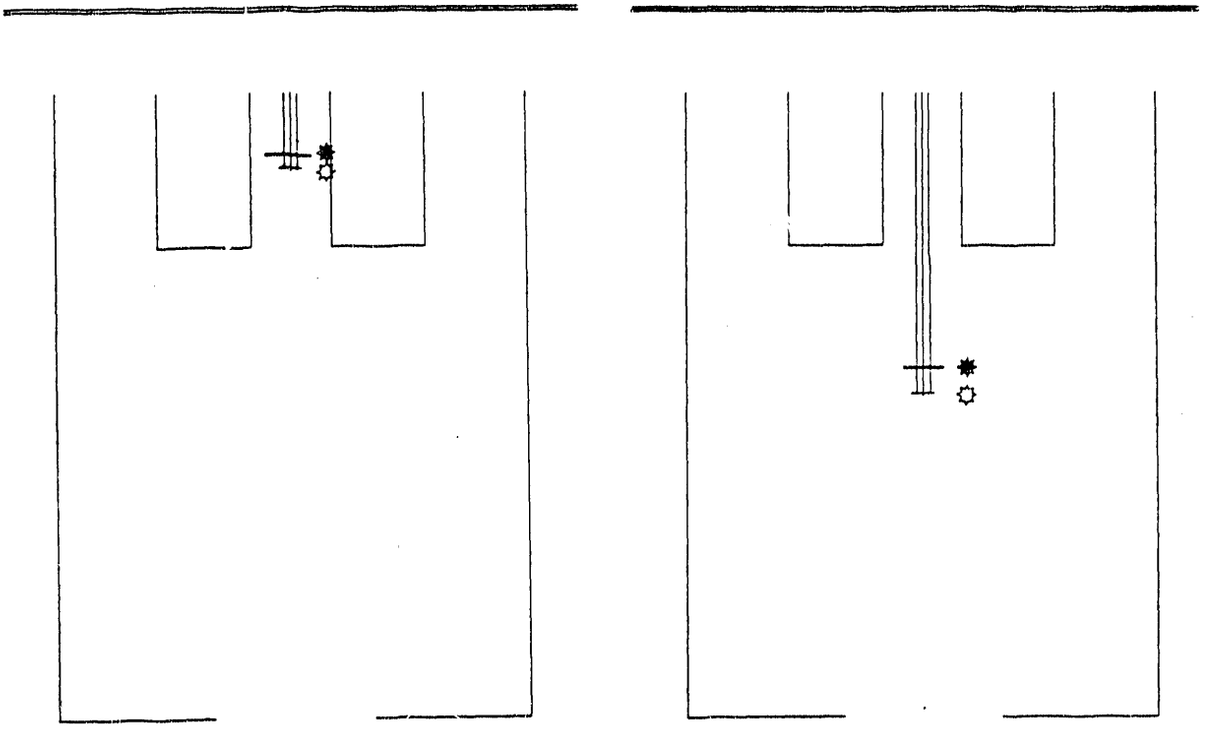

FIGURE 2. Numerical calculations of trajectories of evaporating water (✡) and coal-water (✸) drops of (a) 50μm and (b) 250μm water drops. Injector flowrates at 0.1 lpm, furnace flowrate at 2.0 lpm, wall temperature 1500 K. Scale is expanded 2.5 times in the radial direction.

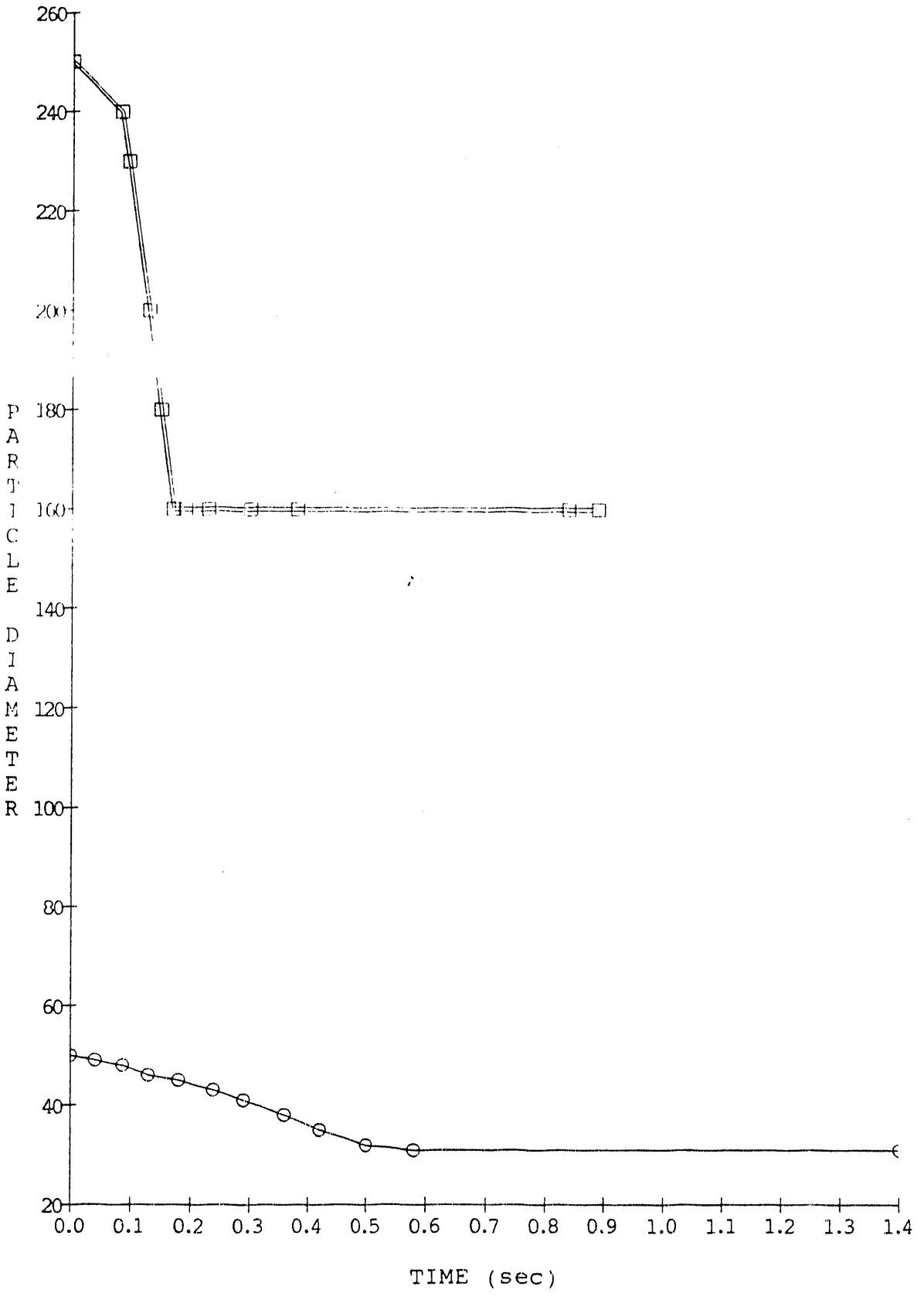

FIGURE 3. Change of the particle diameter of a slurry drop with time, ○250μm and □250μm initial diameter, 75% water - 25% inert solid drops. Injector flowrate 0.1 lpm, furnace flowrate at 2.0 lpm, wall temperature 1500 K.

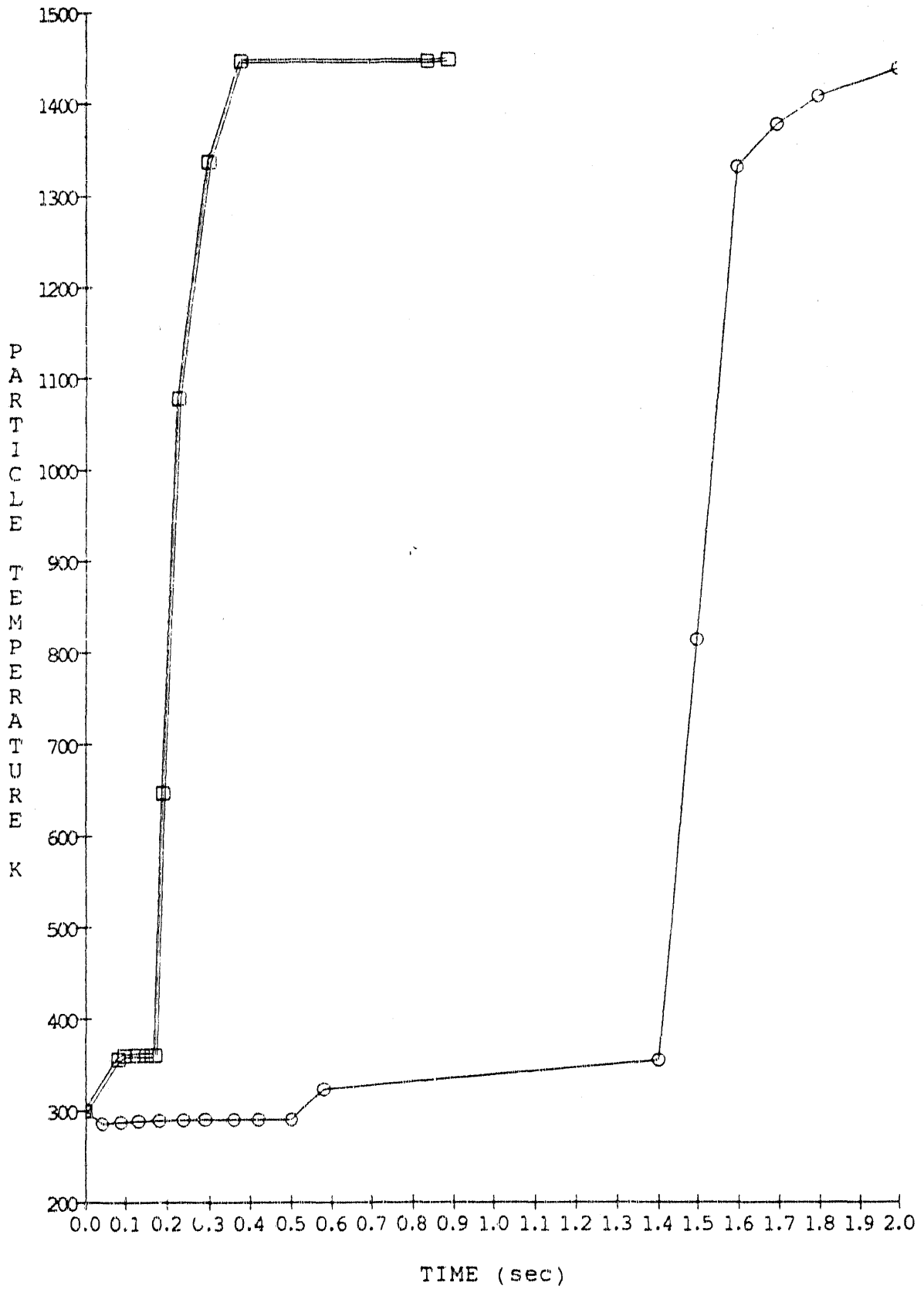

FIGURE 4. Change of the particle temperature of a slurry drop with time, ±50μm and □250μm initial diameter, 75% water - 25% inert solid drops. Injector flowrate 0.1 lpm, furnace flowrate at 2.0 lpm, wall temperature 1500 K.

FIGURE 5. Mechanical plunger-needle drop generator.

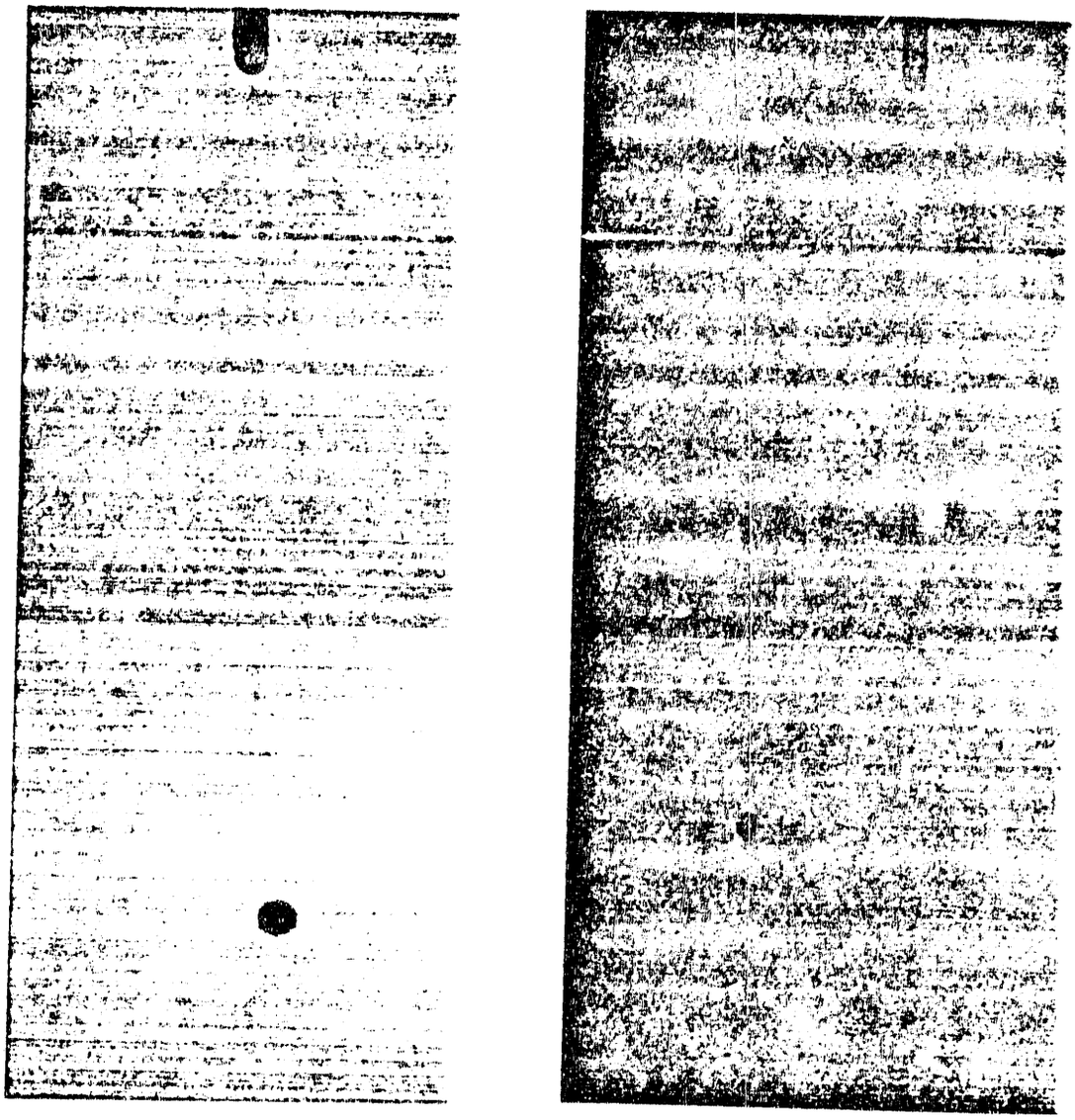

FIGURE 6. Stream droplet generation with the modulation wavelength a. 700μm and b. 400μm.

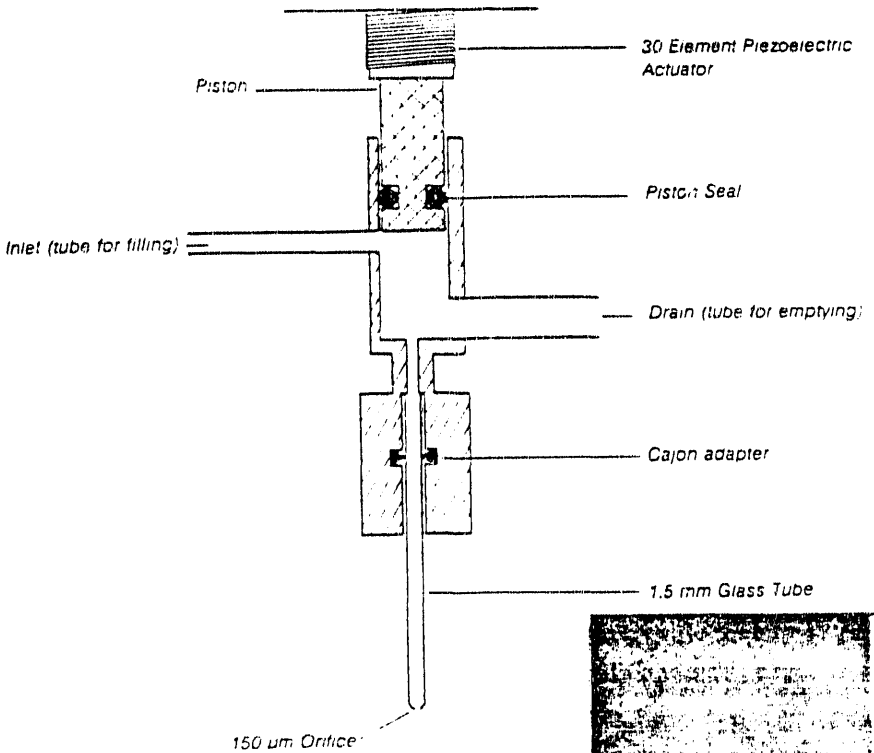

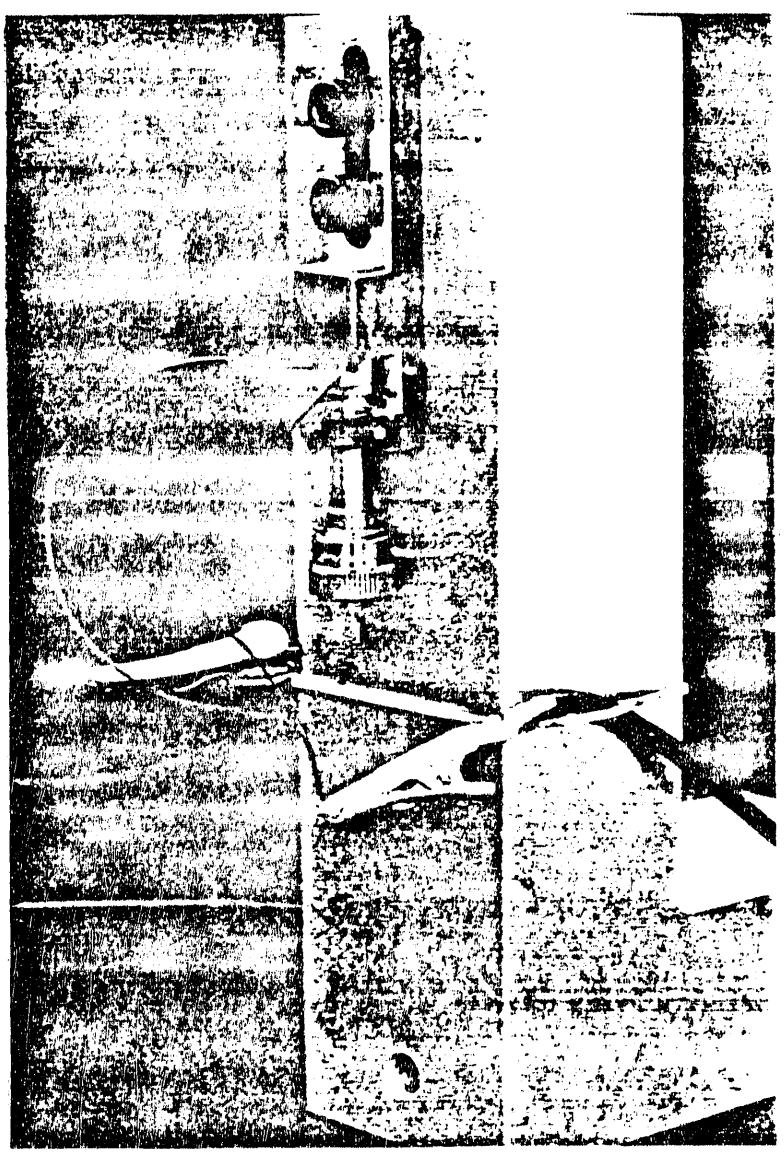

FIGURE 7.

A piezoelectric driven drop generator.

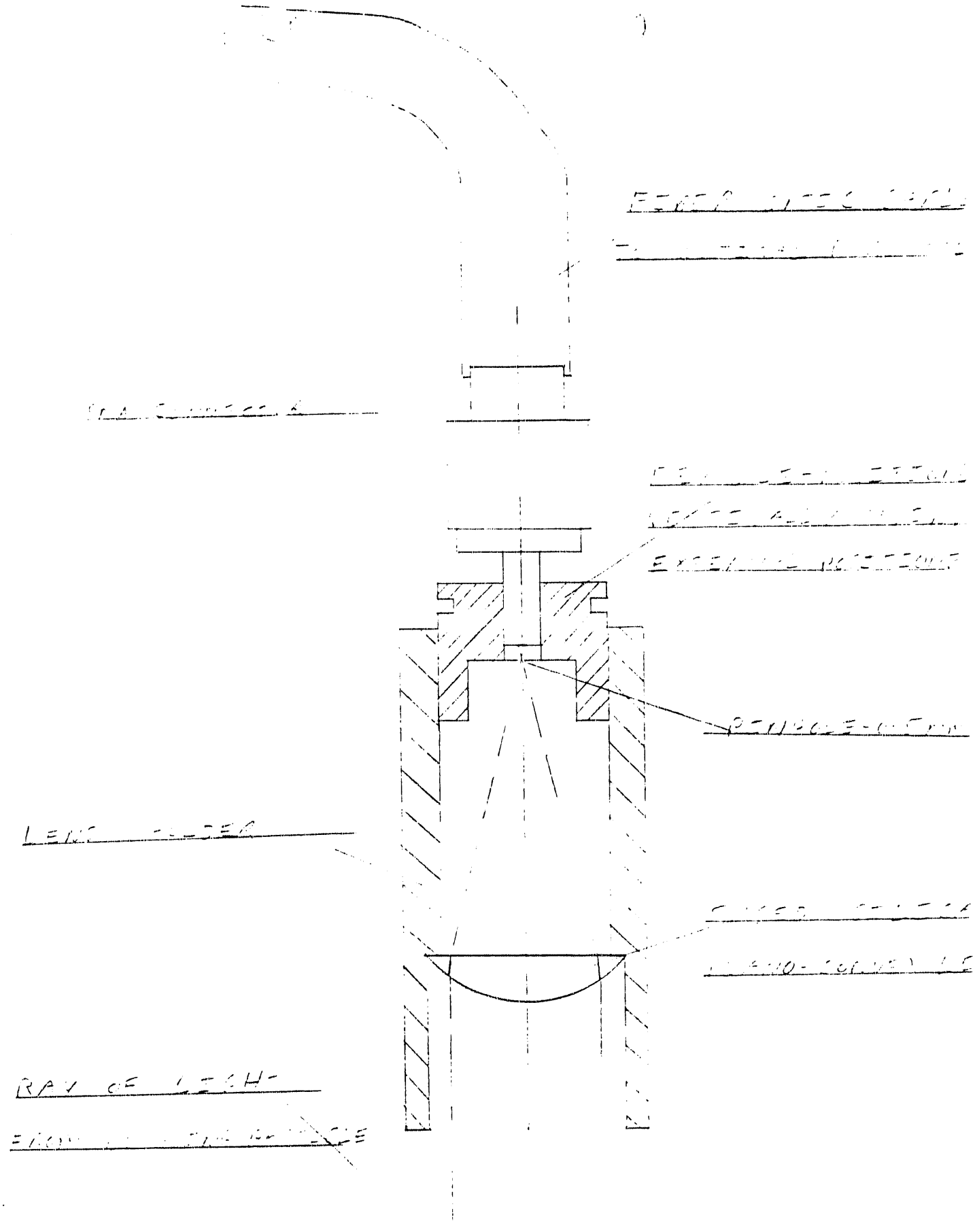

FIGURE 8. Design of the collimating optics.

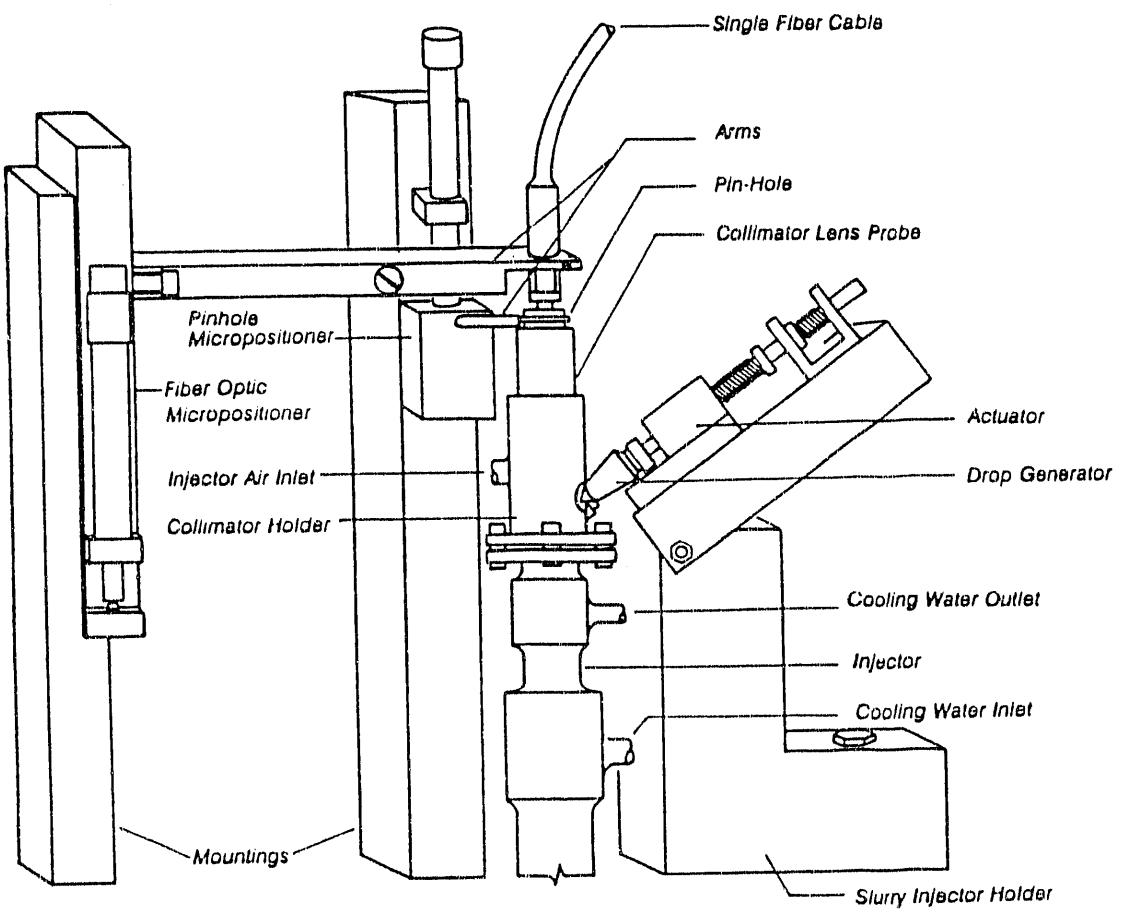

FIGURE 9. Collimating optics-pinhole-fiber optics assembly and the mechanically actuated slurry droplet generator.

END

DATE
FILMED
9/04/92